

Constraints on the anomalous tensor operators from $B \rightarrow \phi K^*, \eta K^*$ and ηK decays

Qin Chang,^{ab} Xin-Qiang Li^{cd} and Ya-Dong Yang^a

^a*Institute of Particle Physics, Huazhong Normal University,
Wuhan, Hubei 430079, P.R. China*

^b*Department of Physics, Henan Normal University,
Xinxiang, Henan 453007, P. R. China*

^c*Institute of Theoretical Physics, Chinese Academy of Sciences,
Beijing, 100080, P. R. China*

^d*Graduate School of the Chinese Academy of Sciences,
Beijing, 100039, P. R. China*

E-mail: changqin1981@163.com, xqli@itp.ac.cn, yangyd@iopp.ccn.edu.cn

ABSTRACT: We investigate whether the anomalous tensor operators with the Lorentz structure $\sigma_{\mu\nu}(1 + \gamma_5) \otimes \sigma^{\mu\nu}(1 + \gamma_5)$, which could provide a simple resolution to the polarization anomaly observed in $B \rightarrow \phi K^*$ decays, could also provide a coherent resolution to the large $\mathcal{B}(B \rightarrow \eta K^*)$ and survive bounds from $B \rightarrow \eta K$ decays. Parameter spaces satisfying all these experimental data are obtained, and found to be dominated by the color-octet tensor operator contribution. Constraints for the equivalent solution with $(1 + \gamma_5) \otimes (1 + \gamma_5)$ operators are also derived and found to be dominated by the color-singlet one. With the constrained parameter spaces, we finally give predictions for $B_s \rightarrow \phi\phi$ decay, which could be tested at the Fermilab Tevatron and the LHC-b experiments.

KEYWORDS: Sum Rules, 1/N Expansion, Chiral Lagrangians.

Contents

1. Introduction	1
2. Theoretical Framework	3
2.1 The SM results within the QCDF framework	3
2.2 Anomalous tensor operators and their contributions to the decay amplitudes	4
2.3 The branching ratios and polarization fractions	7
3. Numerical analysis and discussions	8
3.1 Constraints on the NP parameters from $B^{0,+} \rightarrow \eta K^{(*0,+}$ decays	8
3.2 Constraints on the NP parameters from $B^0 \rightarrow \phi K^{*0}$ decay	10
3.3 Final allowed regions for NP parameters and predictions for $B_s \rightarrow \phi\phi$ decay	13
4. Conclusions	15
A. Decay amplitudes in the SM with QCDF	16
B. Theoretical input parameters	17
B.1 Wilson coefficients and CKM matrix elements	17
B.2 Quark masses and lifetimes	17
B.3 The decay constants and form factors	18
B.4 The LCDAs of mesons	18

1. Introduction

Looking for signals of physics beyond the Standard Model (SM) is one of the most important missions of high energy physics. Complementary to direct searches for new physics (NP) particles in the high energy colliders, the study of B physics is of great importance for probing indirect signals of NP. In this respect, the B factories at SLAC and KEK are doing a commendable job by providing us with a huge amount of data on various B -meson decays, which are mostly in perfect agreement with the SM predictions. However, there still exist some unexplained puzzles, such as the unmatched CP asymmetries in $B \rightarrow \pi K$ decays [1–3], the abnormally large branching ratios of $B \rightarrow \eta' K$ and $B \rightarrow \eta K^*$ decays [1, 2, 4–10], and the large transverse polarization fractions in $B \rightarrow \phi K^*$ decays [1, 2, 11–15, 17–20]. Confronted with these anomalies, we are forced not only to consider more precise QCD effects, but also to speculate on the existence of possible NP scenarios beyond the SM.

It is well-known that the flavor-changing neutral current (FCNC) processes arise only from loop effects within the SM, and are therefore very sensitive to various NP effects.

Since the puzzling B -meson decay processes mentioned above are all related to the FCNC $b \rightarrow s$ transitions, these decay channels could be used as effective probes of possible NP scenarios. So, if one kind of NP could resolve one of these puzzles, it is necessary to investigate whether the same scenario can also provide a simultaneous resolution to the others. Considering the fact that current theoretical estimations of $\mathcal{B}(B \rightarrow \eta'K)$ still suffer from large uncertainties [9, 21], and the NP scenario with anomalous tensor operators considered in this paper do not contribute to the $B \rightarrow \phi K$ and $B \rightarrow \pi K$ decays in the naive factorization (NF) approximation, we shall only focus on the $B \rightarrow \eta K^{(*)}$ and $B \rightarrow \phi K^*$ decays.

The recent experimental data on the longitudinal polarization fraction f_L in $B^0 \rightarrow \phi K^{*0}$ decay is given as

$$f_L = \begin{cases} 0.52 \pm 0.05 \pm 0.02 & \text{BABAR [11],} \\ 0.45 \pm 0.05 \pm 0.02 & \text{Belle [12],} \\ 0.57 \pm 0.10 \pm 0.05 & \text{CDF [13].} \end{cases} \quad (1.1)$$

On the other hand, since the two final-state light vector mesons ϕ and K^{*0} in this decay mode are flying out fleetly in the rest frame of B meson, and the structure of the charged weak interaction current of the SM is left-handed, as well as the fact that high-energy QCD interactions conserve helicity, any spin flip of a fast flying quark will be suppressed by one power of $1/m_b$, with m_b the b quark mass. It is therefore expected that, within the SM, both of the final-state hadrons in this decay mode are mainly longitudinally polarized, with

$$f_L \sim 1 - \mathcal{O}(1/m_b^2), \quad (1.2)$$

while the transverse parts are suppressed by powers of $m_{\phi, K^*}/m_B$. Obviously, the experimental data eq. (1.1) deviates significantly from the SM prediction eq. (1.2), and this polarization anomaly has attracted much interest in searching for possible theoretical explanations both within the SM and in various NP models [14, 17–20]. For example, the authors in refs. [17–20] have studied this anomaly and found that the four-quark tensor operators of the form $\bar{s}\sigma_{\mu\nu}(1 + \gamma_5)b \otimes \bar{s}\sigma^{\mu\nu}(1 + \gamma_5)s$ could offer a simple resolution to the observed polarization anomaly within some possible parameter spaces.

Since the $B \rightarrow \eta K^{(*)}$ decays, in analogy with the $B \rightarrow \phi K^*$ decays, also involve the $b \rightarrow s\bar{s}s$ transition, it is necessary to investigate the effects of these new types of four-quark tensor operators on the latter. In particular, it is very interesting to see whether these new four-quark tensor operators with the same parameter spaces could also simultaneously account for the measured $\mathcal{B}(B \rightarrow \eta K^*)$ [2, 4–6], which are much larger than the theoretical predictions within the SM [8, 9], and survive bounds from $B \rightarrow \eta K$ decays. Motivated by these speculations, in this paper, we shall investigate the effects of the following two types of tensor operators on these decay modes (with i, j the color indices)

$$O_{T1} = \bar{s}\sigma_{\mu\nu}(1 + \gamma_5)b \otimes \bar{s}\sigma^{\mu\nu}(1 + \gamma_5)s, \quad O_{T8} = \bar{s}_i\sigma_{\mu\nu}(1 + \gamma_5)b_j \otimes \bar{s}_j\sigma^{\mu\nu}(1 + \gamma_5)s_i, \quad (1.3)$$

and try to find out the allowed parameter spaces characterized by the strengths and phases of these new tensor operators that satisfy all the experimental constraints from these decays.

Moreover, since the (pseudo-)scalar operators

$$O_{S+P} = \bar{s}(1 + \gamma_5)b \otimes \bar{s}(1 + \gamma_5)s, \quad O'_{S+P} = \bar{s}_i(1 + \gamma_5)b_j \otimes \bar{s}_j(1 + \gamma_5)s_i, \quad (1.4)$$

can be expressed, through the Fierz transformations, as linear combinations of the new tensor operators eq. (1.3), constraints on these two operators can be derived easily from those on the latter.

To further test such a particular NP scenario with anomalous tensor operators, we also give predictions for the branching ratio and the longitudinal polarization fraction of $B_s \rightarrow \phi\phi$ decay, which is also involved the same quark level $b \rightarrow s\bar{s}s$ transition. All these results could be tested at the Fermilab Tevatron and the LHC-b experiments.

The paper is organized as follows. section 2 is devoted to the theoretical framework. After a brief entertainment of the QCD factorization formalism (QCDF) [22], we discuss the anomalous tensor operator contributions to the $B \rightarrow \eta K^{(*)}$ and $B \rightarrow \phi K^*$ decays. In section 3, our numerical analysis and discussions are presented. Section 4 contains our conclusions. Appendix A recapitulates the amplitudes for the five decay modes within the SM [15, 23]. All the theoretical input parameters relevant to our analysis are summarized in appendix B.

2. Theoretical Framework

2.1 The SM results within the QCDF framework

In the SM, the effective Hamiltonian responsible for $b \rightarrow s$ transitions is given as [24]

$$\mathcal{H}_{\text{eff}} = \frac{G_F}{\sqrt{2}} \left[V_{ub}V_{us}^* (C_1 O_1^u + C_2 O_2^u) + V_{cb}V_{cs}^* (C_1 O_1^c + C_2 O_2^c) - V_{tb}V_{ts}^* \left(\sum_{i=3}^{10} C_i O_i + C_{7\gamma} O_{7\gamma} + C_{8g} O_{8g} \right) \right] + \text{h.c.}, \quad (2.1)$$

where $V_{qb}V_{qs}^*$ ($q = u, c$ and t) are products of the Cabibbo-Kobayashi-Maskawa (CKM) matrix elements [25], C_i the Wilson coefficients, and O_i the relevant four-quark operators whose explicit forms could be found, for example, in ref. [22].

In addition to \mathcal{H}_{eff} , we must employ a factorisation formalism of hadronic dynamics to study the $B^- \rightarrow \eta K^-$, $\bar{B}^0 \rightarrow \eta \bar{K}^0$, $B^- \rightarrow \eta K^{*-}$, $\bar{B}^0 \rightarrow \eta \bar{K}^{*0}$, and $\bar{B}^0 \rightarrow \phi \bar{K}^{*0}$ decays. To this end, we take the framework of QCDF [22]. The factorization formula allows us to calculate systemically the hadronic matrix element of operators in the effective Hamiltonian eq. (2.1)

$$\begin{aligned} \langle M_1 M_2 | O_i | B \rangle &= \sum_j F_j^{B \rightarrow M_1} \int_0^1 dx T_{ij}^I(x) \Phi_{M_2}(x) + (M_1 \leftrightarrow M_2) \\ &+ \int_0^1 d\xi \int_0^1 dx \int_0^1 dy T_i^{II}(\xi, x, y) \Phi_B(\xi) \Phi_{M_1}(x) \Phi_{M_2}(y), \end{aligned} \quad (2.2)$$

where $F_j^{B \rightarrow M}$ is the $B \rightarrow M$ transition form factor, T_{ij}^I and T_i^{II} are the perturbatively calculable hard kernels, and $\Phi_X(x)$ ($X = B, M_{1,2}$) are the universal nonperturbative light-cone distribution amplitudes (LCDAs) of the corresponding mesons.

In the recent years, the QCDF formalism has been employed extensively to study non-leptonic B decays. For example, all the decay modes considered here have been studied comprehensively within the SM in refs. [15, 23]. We recapitulate the amplitudes for $B \rightarrow \eta K^{(*)}$ and $B \rightarrow \phi K^*$ decays in appendix A.

It is noted that, along with its many novel progresses in non-leptonic B decays, the framework contains estimates of some power corrections which can not be computed rigorously. These contributions may be numerically important for realistic B -meson decays, especially for some penguin-dominated decay modes [15, 17, 23, 26]. In fact, there are no reliable methods available at present to *calculate* such contributions. To give *conservative* theoretical predictions, at least, one should leave the associated parameters varying in reasonable regions to show their possible effects. In this work, following closely the treatment made in refs. [23, 27], we will parameterize the end-point divergences associated with these power corrections as

$$\int_0^1 \frac{dx}{x} \rightarrow X_A = e^{i\phi_A} \ln \frac{m_B}{\Lambda_h}, \quad \int_0^1 \frac{dx}{x^2} \rightarrow X_L = \frac{m_B}{\Lambda_h} e^{i\phi_A} - 1. \quad (2.3)$$

In the following numerical calculations, we take the parameter Λ_h and the phase ϕ_A varying in the range $0.2 \sim 0.8$ GeV and $-45^\circ \sim 45^\circ$, respectively.

In our calculation, we have neglected possible intrinsic charm content and anomalous gluon couplings related to the meson η , both of which have been shown to have only marginal effects on the four $B \rightarrow \eta K^{(*)}$ decays [8, 9]. As for the η - η' mixing effects, we shall adopt the Feldmann-Kroll-Stech (FKS) scheme [28] as implemented in ref. [9]. A recent study and comparison of different η - η' mixing schemes has been given in ref. [29].

In the amplitude for $\bar{B}^0 \rightarrow \phi \bar{K}^*$ decay in eq. (A.5), a new power-enhanced electromagnetic penguin contribution to the negative-helicity electroweak penguin coefficient $\alpha_{3,EW}^{p,-}$, as first noted by Beneke, Rohrer and Yang [15], has also been taken into account in our calculation. In a recent comprehensive study of $B \rightarrow VV$ decays [16], it is found that the small f_L could be accommodated within the SM, however, with very large theoretical uncertainties.

2.2 Anomalous tensor operators and their contributions to the decay amplitudes

Since the SM may have difficulties in explaining the large $\mathcal{B}(B \rightarrow \eta K^*)$ and the measured polarization observables in $B \rightarrow \phi K^*$ decays, we shall discuss possible NP resolutions to these observed discrepancies. Specifically, we shall investigate whether these discrepancies could be resolved by introducing two anomalous four-quark tensor operators defined by eq. (1.3).

We write the NP effective Hamiltonian as

$$\mathcal{H}_{\text{eff}}^{\text{NP}} = \frac{G_F}{\sqrt{2}} |V_{ts}| e^{i\delta_T} \left[C_{T1} O_{T1} + C_{T8} O_{T8} \right] + \text{h.c.}, \quad (2.4)$$

with the tensor operators O_{T1} and O_{T8} defined by eq. (1.3). The coefficient $C_{T1(T8)}$ describes the relative interaction strength of the tensor operator $O_{T1(T8)}$, and δ_T is the NP

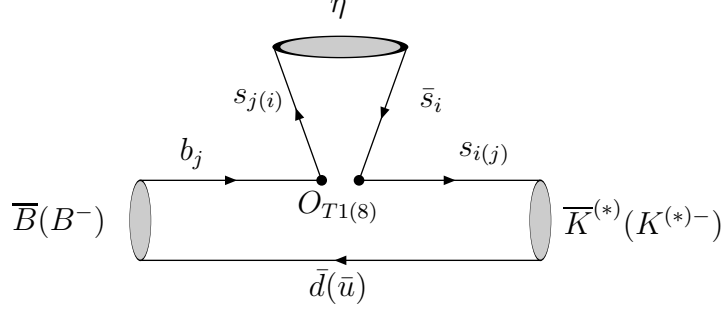


Figure 1: Feynman diagram contributing to the decay amplitudes of $B \rightarrow \eta K^{(*)}$ decays due to the anomalous tensor operators. Another type of insertion has no contribution.

weak phase. In principle, such four-quark tensor operators could be produced in various NP scenarios, e.g., in the Minimal Supersymmetric Standard Model (MSSM) [30, 31]. Interestingly, the recent study of radiative pion decay $\pi^+ \rightarrow e^+ \nu \gamma$ at PIBETA detector [32] has found deviations from the SM predictions in the high- E_γ -low- E_{e^+} kinematic region, which may indicate the existence of anomalous tensor quark-lepton interactions [33–35].

At first, we present the NP contributions to the decay amplitudes of $B \rightarrow \eta K^{(*)}$ and $B \rightarrow \phi K^*$ decays due to these new tensor operators. Since their coefficients are unknown parameters, for simplicity, we shall only consider the leading contributions of these tensor operators.

As for the four $B \rightarrow \eta K^{(*)}$ decays, the relevant Feynman diagram due to the tensor operators $O_{T1, T8}$ is shown in figure 1. It is easy to realize that the amplitude corresponding to another type of insertion would vanish in the leading order approximation. Instead of using the Fierz transformation, an easy way to calculate the amplitude in figure 1 is to use the light-cone projection operator of the meson η in momentum space [23]

$$M_{\alpha\beta}^{\eta_s} = \frac{i f_\eta^s}{4} \left[\not{q} \gamma_5 \Phi_\eta(x) - \mu_{\eta_s} \gamma_5 \frac{k_2 \cdot k_1}{k_2 \cdot k_1} \Phi_p(x) \right]_{\alpha\beta}, \quad (2.5)$$

where q , Φ_η , and Φ_p are the momentum, leading-twist, and twist-3 LCDAs of the meson η , respectively. k_1^μ and k_2^μ denote the momenta of the quark and anti-quark in the meson η , and are given by

$$k_1^\mu = x q^\mu + k_\perp^\mu + \frac{\vec{k}_\perp^2}{2xq \cdot \bar{q}} \bar{q}^\mu, \quad k_2^\mu = \bar{x} q^\mu - k_\perp^\mu + \frac{\vec{k}_\perp^2}{2\bar{x}q \cdot \bar{q}} \bar{q}^\mu, \quad (2.6)$$

with $\bar{x} = 1 - x$, and x the momentum fraction carried by the constituent quark. The decay constant f_η^s and the factor μ_{η_s} in eq. (2.5) are defined, respectively, by [9]

$$\langle \eta(q) | \bar{s} \gamma_\mu \gamma_5 s | 0 \rangle = -i f_\eta^s q_\mu, \quad \mu_{\eta_s} = \frac{\bar{m}_b}{2} r_\chi^{\eta_s} = \frac{h_\eta^s}{2 f_\eta^s \bar{m}_s}, \quad (2.7)$$

where we have used $|\eta\rangle = \cos \phi |\eta_q\rangle - \sin \phi |\eta_s\rangle$, with $|\eta_q\rangle = (|\bar{u}u\rangle + |\bar{d}d\rangle)/\sqrt{2}$ and $|\eta_s\rangle = |\bar{s}s\rangle$ [28].

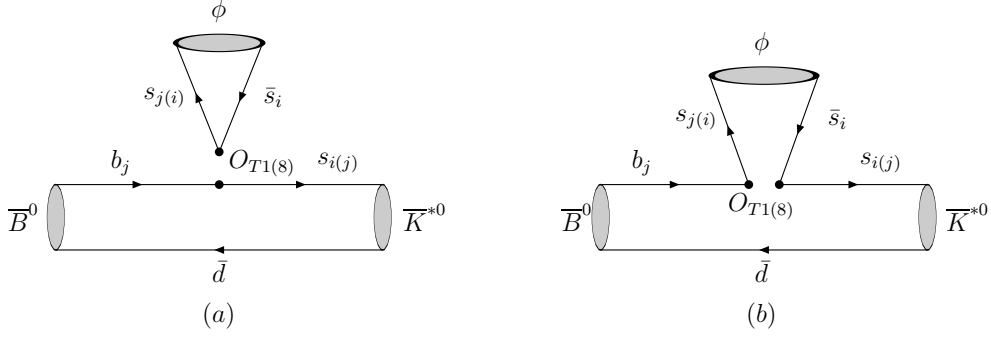


Figure 2: Feynman diagrams contributing to the decay amplitude of $\bar{B}^0 \rightarrow \phi \bar{K}^{*0}$ decay due to the anomalous tensor operators.

After some simple calculations, the NP contributions to the decay amplitudes of the four $B \rightarrow \eta K^{(*)}$ decays due to $\mathcal{H}_{\text{eff}}^{\text{NP}}$ in eq. (2.4) can be written as

$$\mathcal{A}_{B^- \rightarrow \eta K^-}^{\text{NP}} = i \frac{G_F}{\sqrt{2}} |V_{ts}| e^{i\delta_T} 3 g_T r_\chi^{\eta_s} (m_{B_u}^2 - m_{K^-}^2) F_0^{B \rightarrow K}(m_\eta^2) f_\eta^s, \quad (2.8)$$

$$\mathcal{A}_{\bar{B}^0 \rightarrow \eta \bar{K}^0}^{\text{NP}} = i \frac{G_F}{\sqrt{2}} |V_{ts}| e^{i\delta_T} 3 g_T r_\chi^{\eta_s} (m_{B_d}^2 - m_{K^0}^2) F_0^{B \rightarrow K}(m_\eta^2) f_\eta^s, \quad (2.9)$$

$$\mathcal{A}_{B^- \rightarrow \eta K^{*-}}^{\text{NP}} = -i \sqrt{2} G_F |V_{ts}| e^{i\delta_T} 3 g_T r_\chi^{\eta_s} m_{K^{*-}} (\varepsilon_2^* \cdot p) A_0^{B \rightarrow K^*}(m_\eta^2) f_\eta^s, \quad (2.10)$$

$$\mathcal{A}_{\bar{B}^0 \rightarrow \eta \bar{K}^{*0}}^{\text{NP}} = -i \sqrt{2} G_F |V_{ts}| e^{i\delta_T} 3 g_T r_\chi^{\eta_s} m_{K^{*0}} (\varepsilon_2^* \cdot p) A_0^{B \rightarrow K^*}(m_\eta^2) f_\eta^s, \quad (2.11)$$

where $g_T = C_{T8} + C_{T1}/N_c$, and the factor 3 is due to contractions of the involved γ matrices. It is interesting to note that the above four decay amplitudes are all proportional to the “chirally-enhanced” factor $r_\chi^{\eta_s} = \frac{h_\eta^s}{f_\eta^s \bar{m}_b \bar{m}_s}$, which has been found to be very important for charmless hadronic B decays [23].

We now present the NP contribution to the decay amplitude of $\bar{B}^0 \rightarrow \phi \bar{K}^{*0}$ decay. Based on the observation that they contribute only to the transverse polarization amplitudes but not to the longitudinal one [17–19], these anomalous four-quark tensor operators have been proposed to resolve the polarization anomaly observed in $B \rightarrow \phi K^*$ decays. The relevant Feynman diagrams are shown in figure 2. For figure 2 (a), we shall use the following matrix elements [36–38]

$$\begin{aligned} \langle \phi(q, \varepsilon_1) | \bar{s} \sigma^{\mu\nu} s | 0 \rangle &= -f_\phi^T (\varepsilon_{1\perp}^{\mu*} q_\nu - \varepsilon_{1\perp}^{\nu*} q_\mu), \quad (2.12) \\ \langle \bar{K}^*(p', \varepsilon_2) | \bar{s} \sigma_{\mu\nu} q^\nu b | \bar{B}(p) \rangle &= \epsilon_{\mu\nu\rho\sigma} \varepsilon_2^{*\nu} p^\rho p'^\sigma 2T_1^{B \rightarrow K^*}(q^2), \\ \langle \bar{K}^*(p', \varepsilon_2) | \bar{s} \sigma_{\mu\nu} q^\nu \gamma_5 b | \bar{B}(p) \rangle &= (-i) T_2^{B \rightarrow K^*}(q^2) \left\{ \varepsilon_{2,\mu}^* (m_B^2 - m_{K^*}^2) - (\varepsilon_2^* \cdot p) (p + p')_\mu \right\} \\ &\quad + (-i) T_3^{B \rightarrow K^*}(q^2) (\varepsilon_2^* \cdot p) \left\{ q_\mu - \frac{q^2}{m_B^2 - m_{K^*}^2} (p + p')_\mu \right\}. \end{aligned}$$

For figure 2 (b), we shall use the light-cone projector operator of the transversely polarized vector meson ϕ [15, 36]

$$M_\perp^\phi = -\frac{i f_\phi^T}{4} \not{\varepsilon}_{1\perp}^* \not{q} \Phi_\perp(x) + \dots, \quad (2.13)$$

where $\Phi_{\perp}(x)$ is the leading twist LCDA of the meson ϕ , and the ellipsis denotes additional parts that have no contributions in our case. It is easy to find that neither figure 2(a) nor (b) contributes to the longitudinal polarization amplitude, and the final decay amplitude can be written as

$$\begin{aligned} \mathcal{A}_{B^0 \rightarrow \phi \bar{K}^{*0}}^{\text{NP}} = & \frac{G_F}{\sqrt{2}} |V_{ts}| e^{i\delta_T} g'_T (-4i f_{\phi}^T) \left\{ i \epsilon_{\mu\nu\rho\sigma} \epsilon_{1\perp}^{*\mu} \epsilon_2^{*\nu} p^{\rho} p'^{\sigma} 2T_1^{B \rightarrow K^*}(m_{\phi}^2) \right. \\ & + T_2^{B \rightarrow K^*}(m_{\phi}^2) \left[(\epsilon_{1\perp}^* \cdot \epsilon_2^*) (m_B^2 - m_{K^*}^2) - 2(\epsilon_{1\perp}^* \cdot p)(\epsilon_2^* \cdot p) \right] \\ & \left. - 2T_3^{B \rightarrow K^*}(m_{\phi}^2) \frac{m_{\phi}^2}{m_B^2 - m_{K^*}^2} (\epsilon_{1\perp}^* \cdot p)(\epsilon_2^* \cdot p) \right\}, \end{aligned} \quad (2.14)$$

with $g'_T = (1 + \frac{1}{2N_c}) C_{T1} + (\frac{1}{2} + \frac{1}{N_c}) C_{T8}$. In the helicity basis, the new decay amplitude eq. (2.14) can be further decomposed into

$$H_{00}^{\text{NP}} = 0, \quad (2.15)$$

$$H_{\pm\pm}^{\text{NP}} = \frac{G_F}{\sqrt{2}} |V_{ts}| e^{i\delta_T} g'_T (4i f_{\phi}^T) \left[(m_{B_d}^2 - m_{K^{*0}}^2) T_2^{B \rightarrow K^*}(m_{\phi}^2) \mp 2m_{B_d} p_c T_1^{B \rightarrow K^*}(m_{\phi}^2) \right], \quad (2.16)$$

where p_c is the center-of-mass momentum of final mesons in \bar{B}^0 rest frame. Compared with the SM predictions eqs. (A.6) and (A.7), the new transverse polarization amplitudes $H_{\pm\pm}^{\text{NP}}$ are enhanced by a factor of m_{B_d}/m_{ϕ} , while the longitudinal part remains unchanged. It is therefore expected that these new tensor operators might provide a possible resolution to the polarization anomaly observed in $B \rightarrow \phi K^*$ decays.

2.3 The branching ratios and polarization fractions

From the above discussions, the total decay amplitudes are then given as

$$\mathcal{A} = \mathcal{A}^{\text{SM}} + \mathcal{A}^{\text{NP}}, \quad (2.17)$$

where \mathcal{A}^{SM} denotes the SM results obtained using the QCDF, and \mathcal{A}^{NP} the contributions of the particular NP scenario with anomalous tensor operators in eq. (2.4). The corresponding branching ratios are

$$\mathcal{B}(B^{0,+} \rightarrow \eta K^{(*)0,+}) = \frac{\tau_B p_c}{8\pi m_B^2} |\mathcal{A}(B^{0,+} \rightarrow \eta K^{(*)0,+})|^2, \quad (2.18)$$

$$\mathcal{B}(\bar{B}^0 \rightarrow \phi \bar{K}^{*0}) = \frac{\tau_B p_c}{8\pi m_B^2} (|H_{00}|^2 + |H_{++}|^2 + |H_{--}|^2), \quad (2.19)$$

where τ_B is the life time of B meson.

In the transversity basis [39], the decay amplitude for any $\bar{B} \rightarrow VV$ decay can also be decomposed into another three quantities A_0 , A_{\parallel} , and A_{\perp} , which are related to the helicity amplitudes H_{00} , H_{++} , and H_{--} through

$$A_0 = H_{00}, \quad A_{\parallel} = \frac{H_{++} + H_{--}}{\sqrt{2}}, \quad A_{\perp} = -\frac{H_{++} - H_{--}}{\sqrt{2}}. \quad (2.20)$$

In terms of these quantities, we can express the longitudinal polarization fraction as

$$\begin{aligned}
 f_L &= \frac{|A_0|^2}{|A_0|^2 + |A_{\parallel}|^2 + |A_{\perp}|^2} \\
 &= \frac{|H_{00}|^2}{|H_{00}|^2 + |H_{++}|^2 + |H_{--}|^2}.
 \end{aligned}
 \tag{2.21}$$

In addition, the relative phases between these helicity amplitudes $\phi_{\parallel,\perp} = \text{Arg}(A_{\parallel,\perp}/A_0) + \pi$ (the definition of these observables is compatible with that used by the BABAR and Belle collaborations [11, 12]), are potentially very useful for constraining the parameter spaces of NP scenario, however, depend on whether the strong phases of the helicity amplitudes could be calculated reliably.

3. Numerical analysis and discussions

With the theoretical formulas and the input parameters summarized in appendix B for the decay modes of our concerns, we now go to our numerical analysis and discussions.

As shown by the NP decay amplitudes eqs. (2.8)–(2.11) and (2.15)–(2.16), the allowed regions for the parameters g_T and δ_T can be obtained from the four measured $\mathcal{B}(B^{0,+} \rightarrow \eta K^{(*)0,+})$, and the ones for g'_T from $\mathcal{B}(B^0 \rightarrow \phi K^{*0})$ and f_L , respectively. Generally, we have five branching ratios and one polarization fraction, but only three free parameters: one NP weak phase δ_T and two effective coefficients g_T and g'_T (or equivalently C_{T1} and C_{T8}). So, it is easy to guess that these decays could severely constrain or rule out the NP scenario with two anomalous tensor operators eq. (2.4).

To make the guess clear, we shall first find out the allowed regions for the parameters g_T and δ_T from the four $B^{0,+} \rightarrow \eta K^{(*)0,+}$ decays. Then, using the allowed regions for the weak phase δ_T , we try to put constraint on the parameter g'_T from $\mathcal{B}(B^0 \rightarrow \phi K^{*0})$ and f_L . Finally, we can obtain the allowed parameter spaces, if there are, for C_{T1} , C_{T8} , and δ_T that satisfy all the experimental data on the decay modes of our concerns. To further test the particular NP scenario eq. (2.4), we also present our theoretical predictions for $B_s \rightarrow \phi\phi$ decay. Theoretical estimations of the annihilation contributions at present suffer from very large uncertainties, which of course will dilute the requirement of NP very much. To show the dilution, we will give our numerical results for two cases, i.e., with and without annihilations for comparison.

3.1 Constraints on the NP parameters from $B^{0,+} \rightarrow \eta K^{(*)0,+}$ decays

Since the tensor operator contributions to the decay amplitudes of the four $B^{0,+} \rightarrow \eta K^{(*)0,+}$ decays are all characterized by the parameters g_T and δ_T , possible regions for these two NP parameters can be obtained from the measured branching ratios of $B^{0,+} \rightarrow \eta K^{(*)0,+}$ decays. Our main results are shown in tables 1–2 and figures 3–4. The experimental data listed in table 1 are taken from the Heavy Flavor Averaging Group (HFAG) [2]. The SM predictions for the branching ratios of these four decays are presented in the third column of table 1, where the theoretical uncertainties are obtained by varying the input parameters

Decay channel	Experiment	SM	Case I	Case II
$B^- \rightarrow \eta K^-$	2.2 ± 0.3	$2.21^{+1.35}_{-0.85}$	$2.29^{+0.12}_{-0.18}$	$2.19^{+0.35}_{-0.33}$
$B^0 \rightarrow \eta K^0$	< 1.9	1.80 ± 0.82	2.19 ± 0.27	2.17 ± 0.34
$B^- \rightarrow \eta K^{*-}$	$19.5^{+1.6}_{-1.5}$	$1.34^{+1.09}_{-0.65}$	$1.30^{+0.14}_{-0.14}$	$1.25^{+0.31}_{-0.28}$
$B^0 \rightarrow \eta K^{*0}$	16.1 ± 1.0	1.02 ± 0.65	1.42 ± 0.22	1.34 ± 0.30
		$6.27^{+3.4}_{-2.3}$	$18.15^{+0.21}_{-0.09}$	$17.44^{+0.68}_{-0.55}$
		5.03 ± 1.82	17.88 ± 0.49	17.45 ± 0.61
		$6.87^{+3.5}_{-2.5}$	$16.96^{+0.09}_{-0.16}$	$17.13^{+0.56}_{-0.68}$
		5.60 ± 1.95	17.10 ± 0.29	17.03 ± 0.65

Table 1: Experimental data [2] and theoretical predictions for the branching ratios (in units of 10^{-6}). The numbers in columns Case I and Case II are our fitting results with g_T and δ_T constrained by varying the experimental data within 1σ and 2σ error bars, respectively. For each decay mode, the first (second) row is evaluated with(out) the annihilation contributions.

within the regions specified in eq. (2.3) and appendix B. For each decay mode, the first and the second row are evaluated with and without the annihilation contributions, respectively.

From table 1, we can see that the theoretical predictions within the SM for both $\mathcal{B}(B^- \rightarrow \eta K^-)$ and $\mathcal{B}(B^0 \rightarrow \eta K^0)$ agree with the experimental data within errors. However, both $\mathcal{B}(B^- \rightarrow \eta K^{*-})$ and $\mathcal{B}(B^0 \rightarrow \eta K^{*0})$ are quite lower than the experimental data. We also note that our results are a little different with those in refs. [8, 9, 23], due to different choices for the input parameters, such as the moderate strength of X_A , λ_B , and so on.

As shown in figure 3, the four $\mathcal{B}(B^{0,+} \rightarrow \eta K^{(*)0,+})$ are very sensitive to the presence of the $\mathcal{H}_{\text{eff}}^{NP}$ of eq. (2.4). The two bands for the parameter spaces constrained by $B^- \rightarrow \eta K^-$ and $B^0 \rightarrow \eta K^0$ decays are much overlapped, and the same situation is also found for the two bands constrained by $B^- \rightarrow \eta K^{*-}$ and $B^0 \rightarrow \eta K^{*0}$ decays. However, we note that $\mathcal{B}(B \rightarrow \eta K)$ and $\mathcal{B}(B \rightarrow \eta K^*)$ have quite different dependence on these NP contributions. So, the allowed regions for the parameters g_T and δ_T are severely narrowed down when constraints from these four decay modes are combined.

The final allowed regions for the parameters g_T and δ_T extracted from the four $B^{0,+} \rightarrow \eta K^{(*)0,+}$ decays are shown in figure 4, where the left (right) plot is the results with(out) the annihilation contributions. In addition, the dark and the gray regions in figure 4 correspond to the results obtained with the measured branching ratios varying within 1σ and 2σ error bars, respectively. From now on, we denote these two possible regions by Case I and Case II. Comparing the two plots in figure 4, one can find that the uncertainties of annihilation contributions would loosen constraints on the NP parameters, especially on δ_T . The numerical results for the parameters g_T and δ_T corresponding to the above two allowed regions are presented in table 2.

As shown in table 1, with the parameters g_T and δ_T varying within these two allowed regions, the large $\mathcal{B}(B^- \rightarrow \eta K^{*-})$ and $\mathcal{B}(B^0 \rightarrow \eta K^{*0})$ can be accounted for by the anomalous four-quark tensor operators without violating $\mathcal{B}(B^- \rightarrow \eta K^-)$. It is also interesting to note that, taking the 90% CL upper limit of $\mathcal{B}(B^0 \rightarrow \eta K^0)$ as an input, our fitting result

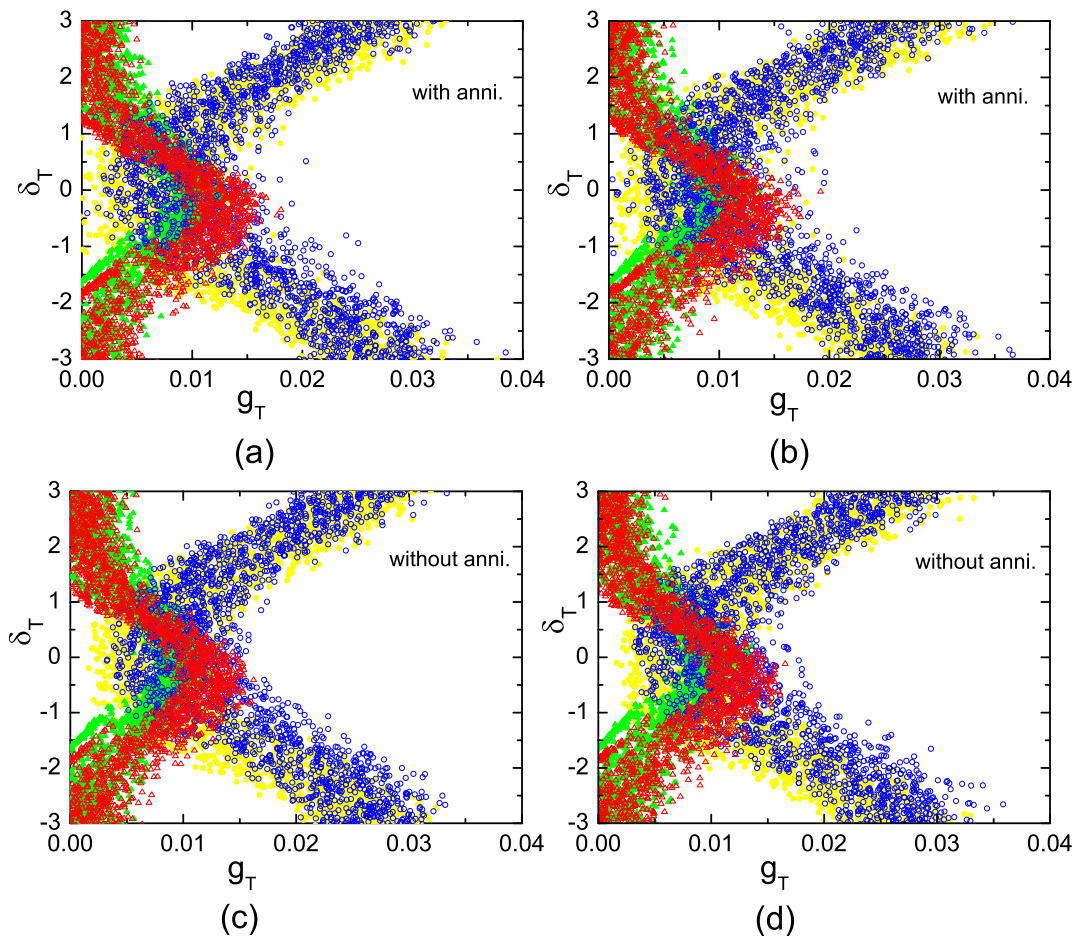


Figure 3: The contour plots for the parameters g_T and δ_T with the experimental data varying within 1σ ((a) and (c)) and 2σ ((b) and (d)) error bars, respectively. The red triangle, green triangle, blue circle, and yellow circle bands come from the decays $B^- \rightarrow \eta K^-$, $B^0 \rightarrow \eta K^0$, $B^- \rightarrow \eta K^{*-}$, and $B^0 \rightarrow \eta K^{*0}$, respectively. Plots labels ‘with(out) anni.’ denote the results with(out) the annihilation contributions.

for $\mathcal{B}(B^0 \rightarrow \eta K^0)$ is in good agreement with the very recent measurements

$$\mathcal{B}(B^0 \rightarrow \eta K^0) = (1.8_{-0.6}^{+0.7} \pm 0.1) \times 10^{-6} \quad \text{BABAR [5]}, \quad (3.1)$$

$$\mathcal{B}(B^0 \rightarrow \eta K^0) = (1.1 \pm 0.4 \pm 0.1) \times 10^{-6} \quad \text{Belle [6]}, \quad (3.2)$$

which give the average value $\mathcal{B}(B^0 \rightarrow \eta K^0) = (1.3 \pm 0.3) \times 10^{-6}$.

3.2 Constraints on the NP parameters from $B^0 \rightarrow \phi K^{*0}$ decay

Now we discuss constraints on the NP parameters from $B^0 \rightarrow \phi K^{*0}$ decay. With the NP weak phase δ_T already extracted from the four $B^{0,+} \rightarrow \eta K^{(*)0,+}$ decays, the parameter g'_T could be severely constrained by the well measured $\mathcal{B}(B^0 \rightarrow \phi K^{*0})$ and f_L . Our results are presented in table 3, figures 5 and 6.

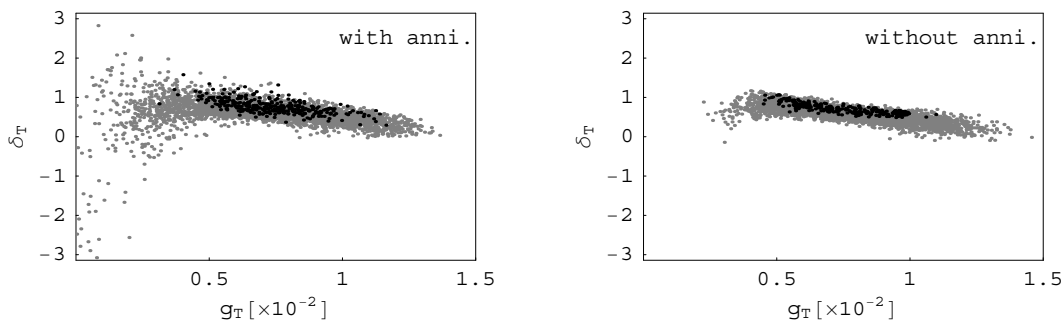


Figure 4: The allowed regions for the parameters g_T and δ_T constrained by the four $B^{0,+} \rightarrow \eta K^{(*)0,+}$ decays. The dark and the gray regions correspond to the results obtained with the measured branching ratios varying within 1σ and 2σ error bars, respectively. The left (right) plot denotes the results with(out) the annihilation contributions.

	Allowed region	$g_T (\times 10^{-3})$	$g'_T (\times 10^{-3})$	$\delta_T (\text{rad})$
Case I	dark	$7.3^{+1.6}_{-1.5}$	$7.6^{+1.0}_{-0.9}$	$0.77^{+0.20}_{-0.16}$
		7.7 ± 1.6	8.9 ± 0.5	0.70 ± 0.13
Case II	gray	$7.2^{+2.5}_{-2.8}$	$8.3^{+1.3}_{-1.2}$	$0.60^{+0.29}_{-0.39}$
		8.0 ± 2.3	9.1 ± 0.6	0.55 ± 0.20

Table 2: The numerical results for the parameters g_T and δ_T , corresponding to the two allowed regions shown in figure 4. The allowed regions for the parameter g'_T constrained by $B^0 \rightarrow \phi K^{*0}$ decay are also presented. For each case, the first (second) row denotes the results with(out) the annihilation contributions.

Observable	Experiment	SM	Case I	Case II
$\mathcal{B} (\times 10^{-6})$	9.5 ± 0.9	$5.9^{+1.2}_{-1.0}$	$9.6^{+0.5}_{-0.6}$	$9.9^{+0.8}_{-1.1}$
		5.7 ± 0.6	10.0 ± 0.3	10.3 ± 0.7
f_L	0.49 ± 0.04	$0.76^{+0.06}_{-0.07}$	$0.50^{+0.02}_{-0.02}$	$0.54^{+0.02}_{-0.03}$
		0.78 ± 0.03	0.52 ± 0.01	0.55 ± 0.01
$\phi_{\parallel} (\text{rad})$	$2.41^{+0.18}_{-0.16}$	$2.90^{+0.25}_{-0.27}$	$1.95^{+0.13}_{-0.12}$	$1.81^{+0.34}_{-0.18}$
		2.91 ± 0.01	1.82 ± 0.05	1.72 ± 0.08
$\phi_{\perp} (\text{rad})$	2.52 ± 0.17	$2.90^{+0.25}_{-0.27}$	$1.96^{+0.13}_{-0.12}$	$1.83^{+0.38}_{-0.18}$
		2.91 ± 0.01	1.82 ± 0.05	1.73 ± 0.08

Table 3: Experimental data [2] and theoretical predictions for the observables in $B^0 \rightarrow \phi K^{*0}$ decay. The other captions are the same as in table 1.

From table 3, we can see that, with our choice for the input parameters, especially our quite optimistic choice for the annihilation contributions, the SM predictions for both $\mathcal{B}(B^0 \rightarrow \phi K^{*0})$ and f_L deviate from the experimental data, and possible NP scenarios beyond the SM may be needed to resolve the observed polarization anomaly.

Figure 5 shows the dependence of $\mathcal{B}(B^0 \rightarrow \phi K^{*0})$ and f_L on the parameter g'_T , with the NP weak phase δ_T extracted from the four $B^{0,+} \rightarrow \eta K^{(*)0,+}$ decays. To illuminate

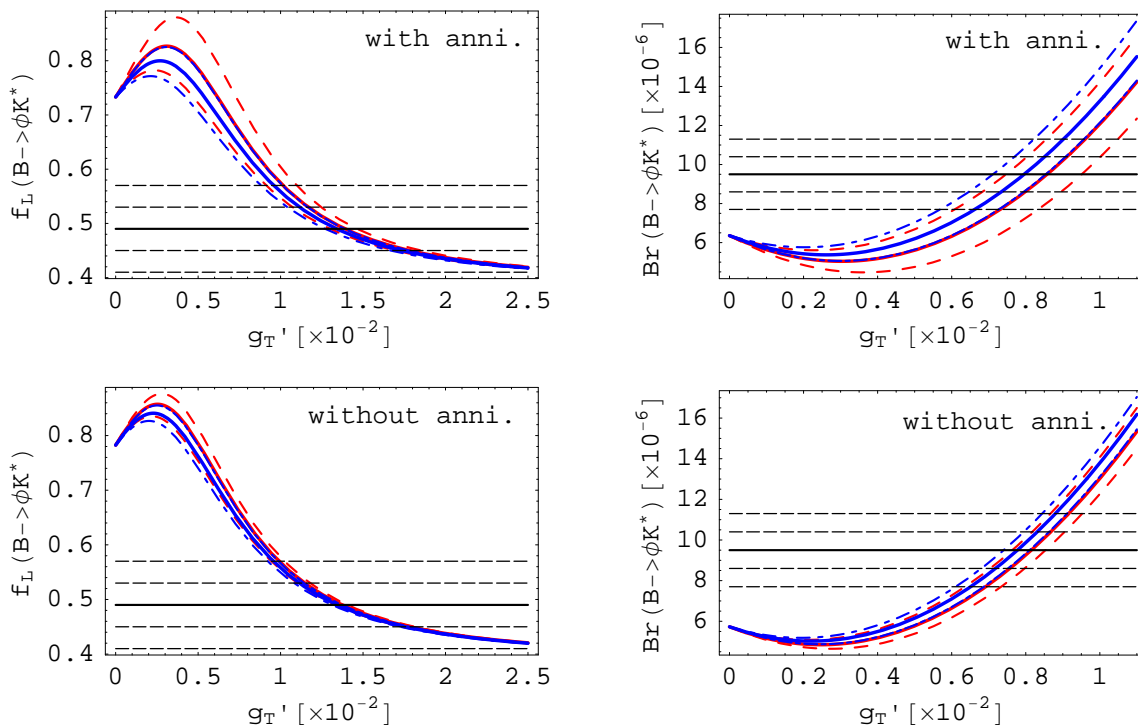


Figure 5: The dependence of $\mathcal{B}(B^0 \rightarrow \phi K^{*0})$ and $f_L(B^0 \rightarrow \phi K^{*0})$ on the parameter g_T' with the NP weak phase δ_T extracted from the four $B^{0,+} \rightarrow \eta K^{(*)0,+}$ decays. The upper and the lower plots denote the results with and without the annihilation contributions, respectively. In each plots, the solid blue (red) curves are the results with δ_T given by Case I (II), and dashed curves due to the error bars of this parameter. The horizontal lines are the experimental data with the solid lines being the central values and the dashed ones the error bars (1σ and 2σ).

the dependence more clearly, we have taken all the other input parameters to be their center values. As shown in figure 5, both $\mathcal{B}(B^0 \rightarrow \phi K^{*0})$ and f_L are very sensitive to the parameter g_T' . It is particularly interesting to note that the variation trends of these two observables relative to the parameter g_T' are opposite to each other. Thus, with the allowed regions for the NP weak phase δ_T extracted from the four $B^{0,+} \rightarrow \eta K^{(*)0,+}$ decays, and the experimental data on these two observables, we could get constraints on the parameter g_T' . The final allowed regions for the parameters g_T' and δ_T are shown in figure 6, with the corresponding numerical results given in table 2.

Corresponding to the two allowed regions for the parameters g_T' and δ_T given in table 2, both $\mathcal{B}(B^0 \rightarrow \phi K^{*0})$ and f_L are in good agreement with the experimental data as shown in table 3. On the other hand, without the annihilation contributions, our predictions for the relative phases ϕ_{\parallel} and ϕ_{\perp} in the decay $B^0 \rightarrow \phi K^{*0}$ are not consistent with the experimental data. This mismatch is, however, reduced by including the annihilation contributions associated with strong phase, which may indicate the annihilation contributions to be complex. We also note that the annihilation contributions have been proved recently to be real and power suppressed [40]. Moreover, in ref. [41], it is found that the NP strong

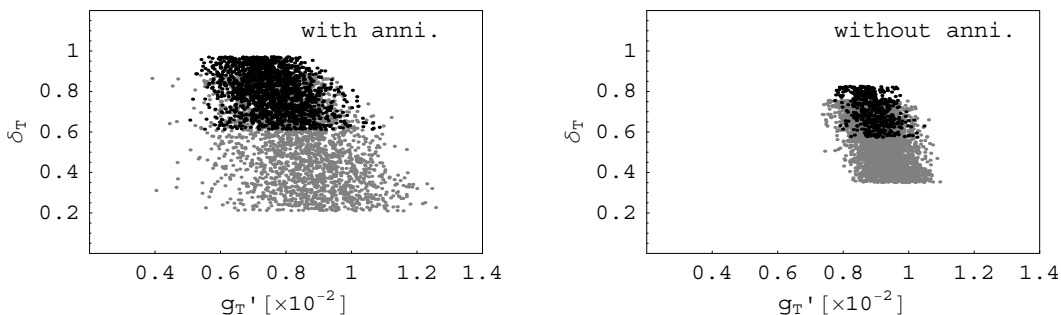


Figure 6: The allowed regions for the parameters g'_T constrained by $\mathcal{B}(B^0 \rightarrow \phi K^{*0})$ and f_L with the NP weak phase δ_T extracted from the four $B^{0,+} \rightarrow \eta K^{(*)0,+}$ decays. Other captions are the same as in figure 4.

	Allowed region	$C_{T1}(\times 10^{-3})$	$C_{T8}(\times 10^{-3})$	$\delta_T(\text{rad})$
Case I	dark	$1.7^{+1.9}_{-1.7}$	$6.8^{+2.2}_{-1.9}$	$0.77^{+0.20}_{-0.16}$
		2.8 ± 1.6	6.7 ± 2.1	0.70 ± 0.13
Case II	gray	$2.6^{+2.8}_{-3.0}$	$6.4^{+3.3}_{-3.7}$	$0.60^{+0.29}_{-0.39}$
		2.8 ± 2.2	7.1 ± 3.0	0.55 ± 0.20

Table 4: Final results for the coefficients C_{T1} , C_{T8} , and the weak phase δ_T extracted from $B \rightarrow \eta K^{(*)}$ and $B^0 \rightarrow \phi K^{*0}$ decays. The other captions are the same as in table 2.

phases are generally negligibly small compared to those of the SM contributions. Further discussion of possible resolution to the mismatch would be beyond the scope of this paper.

3.3 Final allowed regions for NP parameters and predictions for $B_s \rightarrow \phi\phi$ decay

Finally, using the relations

$$g_T = C_{T8} + \frac{C_{T1}}{N_c}, \quad (3.3)$$

$$g'_T = \left(1 + \frac{1}{2N_c}\right) C_{T1} + \left(\frac{1}{2} + \frac{1}{N_c}\right) C_{T8}, \quad (3.4)$$

with $N_c = 3$, we get the final allowed regions for the parameters C_{T1} and C_{T8} , which are presented in table 4. It is interesting to note that the color-octet operator O_{T8} dominates the NP contributions. Actually, with O_{T8} only, we obtain $C_{T8} = (7.3^{+1.6}_{-1.5}) \times 10^{-3}$ ($(7.7 \pm 1.6) \times 10^{-3}$) and $C_{T8} = (9.1^{+1.2}_{-1.0}) \times 10^{-3}$ ($(10.7 \pm 0.6) \times 10^{-3}$) from $B \rightarrow \eta K^{(*)}$ and $B \rightarrow \phi K^*$ decays, respectively, where (also for the following results) the numbers in the bracket are obtained without the annihilation contributions. Thus, we obtain a single color-octet O_{T8} solution with $C_{T8} = (8.5^{+0.9}_{-0.9}) \times 10^{-3}$ ($(10.3 \pm 0.5) \times 10^{-3}$) and $\delta_T = 44.1^{+11.6}_{-9.0}^\circ$ ($40.2^\circ \pm 7.2^\circ$). However, with the color-singlet operator O_{T1} only, we could not get any solution.

It is noted that the two tensor operators O_{T1} and O_{T8} could be expressed by the other two (pseudo-) scalar operators O_{S+P} and O'_{S+P} through the Fierz transformation

Observable	Experiment	SM	Case I	Case II
$\mathcal{B}(\times 10^{-6})$	14_{-7}^{+8}	$20.6_{-3.0}^{+4.2}$	$29.4_{-3.5}^{+4.4}$	$20.1_{-4.8}^{+5.9}$
		17 ± 2	30 ± 3	29 ± 3
f_L	—	$0.83_{-0.06}^{+0.04}$	$0.73_{-0.08}^{+0.07}$	$0.72_{-0.07}^{+0.07}$
		0.83 ± 0.02	0.66 ± 0.03	0.67 ± 0.03

Table 5: Theoretical predictions for $B_s \rightarrow \phi\phi$ decay both within the SM and in the particular NP scenario eq. (2.4). The other captions are the same as in table 1.

relations [18]

$$O_{S+P} = \frac{1}{12}O_{T1} - \frac{1}{6}O_{T8}, \quad O'_{S+P} = \frac{1}{12}O_{T8} - \frac{1}{6}O_{T1}. \quad (3.5)$$

Such operators could be generated in many NP scenarios with scalar interactions. It would be useful to present the constraints on the coefficients of the two $(S+P) \otimes (S+P)$ operators. To this end, we get

$$C_{S+P} = (-0.99_{-0.35}^{+0.39}) \times 10^{-3} \quad ((-0.89 \pm 0.38) \times 10^{-3}), \quad (3.6)$$

$$C'_{S+P} = (0.29_{-0.32}^{+0.36}) \times 10^{-3} \quad ((0.09 \pm 0.32) \times 10^{-3}), \quad (3.7)$$

with the normalization factor $\frac{G_F}{\sqrt{2}}|V_{ts}|$ and a new weak phase $\delta_T = 44.1^\circ_{-9.0^\circ}^{+11.6^\circ}$ ($40.2^\circ \pm 7.2^\circ$), corresponding to the two tensor operators case. The single O_{T8} solution would correspond to $C_{S+P} \equiv -2C'_{S+P} = (-1.4_{-0.2}^{+0.1}) \times 10^{-3}$ ($(-1.7 \pm 0.1) \times 10^{-3}$), and the weak phase is the same as the former. It should be noted that the relation $C_{S+P} = -2C'_{S+P}$ is strictly required for the last correspondence.

To further test the particular NP scenario with anomalous tensor operators eq. (2.4), we also present our theoretical predictions for the branching ratio and the longitudinal polarization fraction of $B_s \rightarrow \phi\phi$ decay, as summarized in table 5. Within the SM, its decay amplitude is given by [15]

$$\frac{1}{2}A_{B_s \rightarrow \phi\phi}^{\text{SM}} = A_{\phi\phi} \sum_{p=u,c} V_{pb}V_{ps}^* \left[\alpha_3^{p,h} + \alpha_4^{p,h} - \frac{1}{2}\alpha_{3,\text{EW}}^{p,h} - \frac{1}{2}\alpha_{4,\text{EW}}^{p,h} + \beta_3^{p,h} - \frac{1}{2}\beta_{3,\text{EW}}^{p,h} + \beta_4^{p,h} - \frac{1}{2}\beta_{4,\text{EW}}^{p,h} \right].$$

With respect to the relevant quantities in eq. (3.8), one can get them directly from those for $B^0 \rightarrow \phi K^{*0}$ decay with some simple changes. This decay mode is of particular interest to test the proposed resolutions to the polarization anomalies observed in $B \rightarrow \phi K^*$ decays, since both of these decay modes are mediated by the same quark level subprocess $b \rightarrow s\bar{s}s$. In addition, since the two final-state mesons are identical in this decay mode, more observables in the time-dependent angular analysis will become zero [39]. So, this decay mode can be considered as an ideal probe for various NP scenarios proposed to resolve the polarization anomalies observed in $B \rightarrow \phi K^*$ decays. The earlier studies of this particular decay mode within the QCDF formalism have been carried out in ref. [42], but without taking into account the annihilation contributions.

From the numerical results presented in tables 3 and 5, we can see that both the branching ratio and the longitudinal polarization fraction of $B_s \rightarrow \phi\phi$ decay is larger than those of the decay $B^0 \rightarrow \phi K^{*0}$, which is due to the relative factor of two in the $\phi\phi$ amplitude eq. (3.8), as well as the additional contribution from the annihilation coefficient $\beta_4^{p,h}$. In particular, due to an accidental cancelation, the annihilation coefficient $\beta_3^{p,0}$ (contributing to both $H_{00}(B^0 \rightarrow \phi K^{*0})$ and $H_{00}(B_s \rightarrow \phi\phi)$) is quite smaller than $\beta_4^{p,0}$ [15]. Interestingly, recent calculations made in the perturbative QCD approach also predict a large branching ratio $\mathcal{B}(B_s \rightarrow \phi\phi) = (44.1_{-6.5}^{+8.3+13.3+0.0} / 8.4_{-0.0}) \times 10^{-6}$ with the longitudinal polarization fraction $f_L(B_s \rightarrow \phi\phi) = (68.0_{-4.0}^{+4.2+1.7+0.0} / 2.2_{-0.0}) \times 10^{-2}$ [43]. Their result for $f_L(B_s \rightarrow \phi\phi)$ is smaller than our predictions within the SM. The predicted results presented in table 5 could be tested at the Fermilab Tevatron and the LHC-b experiments.

4. Conclusions

In summary, motivated by the observed discrepancies between the experimental data and the SM predictions for the branching ratios of $B \rightarrow \eta K^*$ decays and the polarization fractions in $B \rightarrow \phi K^*$ decays, we have studied a particular NP scenario with anomalous tensor operators O_{T1} and O_{T8} , which has been proposed to resolve the polarization anomalies in the literature [17–19].

After extensive numerical analysis, we have found that the above observed discrepancies could be resolved simultaneously and constraints on the NP parameters have been obtained. With both the experimental data and the theoretical input parameters varying within 1σ error bars, we have found the following two solutions: (I) both the two tensor operators contribute with the parameter spaces presented in the upper two rows of table 4; (II) only O_{T8} contributes with $C_{T8} = (8.5_{-0.9}^{+0.9}) \times 10^{-3} ((10.3 \pm 0.5) \times 10^{-3})$ and δ_T the same as solution (I). The above two solutions correspond to the scenario with new operators O_{S+P} and O'_{S+P} added to the SM, with the parameter spaces: (I) $C_{S+P} = (-0.99_{-0.35}^{+0.39}) \times 10^{-3} ((-0.89 \pm 0.38) \times 10^{-3})$, $C'_{S+P} = (0.29_{-0.32}^{+0.36}) \times 10^{-3} ((0.09 \pm 0.32) \times 10^{-3})$ and (II) $C_{S+P} \equiv -2C'_{S+P} = (-1.4_{-0.2}^{+0.1}) \times 10^{-3} ((-1.7 \pm 0.1) \times 10^{-3})$. Their weak phase δ_{S+P} is the same as δ_T .

Against our early expectations, we have found that the solution with two tensor operators are dominated by the color-octet operator O_{T8} . It would be interesting to investigate whether the available NP models could give such effective interactions at the m_b scale.

To further test the particular NP scenario with two anomalous tensor operators $O_{T1,T8}$ or (pseudo-) scalar operators $O_{S+P}^{(\prime)}$, we have also presented our predictions for the observables in $B_s \rightarrow \phi\phi$ decay, which could be tested more thoroughly at the Fermilab Tevatron and the LHC-b experiments in the near future.

It should be noted that the strong constraints in table 4 obtained without annihilation contributions may be too optimistic. As has been shown in the table, the uncertainties due to poorly known annihilation contributions could dilute the requirement of NP very much. Generally, this caveat could be applied to probe possible NP scenarios in exclusive non-leptonic B decays. Further theoretical progress is strongly demanded.

Acknowledgments

The work is supported by National Science Foundation under contract Nos. 10305003 and 10675039, and the NCET Program sponsored by Ministry of Education, China.

A. Decay amplitudes in the SM with QCDF

The amplitudes for $B \rightarrow \eta K^{(*)}$ are recapitulated from ref. [23]

$$\begin{aligned} \sqrt{2} \mathcal{A}_{B^- \rightarrow K^- \eta}^{\text{SM}} &= \sum_{p=u,c} V_{pb} V_{ps}^* \left\{ A_{K^- \eta_q} \left[\delta_{pu} \alpha_2 + 2\alpha_3^p + \frac{1}{2} \alpha_{3,\text{EW}}^p \right] \right. \\ &\quad + \sqrt{2} A_{K^- \eta_s} \left[\delta_{pu} \beta_2 + \alpha_3^p + \alpha_4^p - \frac{1}{2} \alpha_{3,\text{EW}}^p - \frac{1}{2} \alpha_{4,\text{EW}}^p + \beta_3^p + \beta_{3,\text{EW}}^p \right] \\ &\quad \left. + A_{\eta_q K^-} \left[\delta_{pu} (\alpha_1 + \beta_2) + \alpha_4^p + \alpha_{4,\text{EW}}^p + \beta_3^p + \beta_{3,\text{EW}}^p \right] \right\}, \end{aligned} \quad (\text{A.1})$$

$$\begin{aligned} \sqrt{2} \mathcal{A}_{B^0 \rightarrow \bar{K}^0 \eta}^{\text{SM}} &= \sum_{p=u,c} V_{pb} V_{ps}^* \left\{ A_{\bar{K}^0 \eta_q} \left[\delta_{pu} \alpha_2 + 2\alpha_3^p + \frac{1}{2} \alpha_{3,\text{EW}}^p \right] \right. \\ &\quad + \sqrt{2} A_{\bar{K}^0 \eta_s} \left[\alpha_3^p + \alpha_4^p - \frac{1}{2} \alpha_{3,\text{EW}}^p - \frac{1}{2} \alpha_{4,\text{EW}}^p + \beta_3^p - \frac{1}{2} \beta_{3,\text{EW}}^p \right] \\ &\quad \left. + A_{\eta_q \bar{K}^0} \left[\alpha_4^p - \frac{1}{2} \alpha_{4,\text{EW}}^p + \beta_3^p - \frac{1}{2} \beta_{3,\text{EW}}^p \right] \right\}, \end{aligned} \quad (\text{A.2})$$

$$\begin{aligned} \sqrt{2} \mathcal{A}_{B^- \rightarrow K^{*-} \eta}^{\text{SM}} &= \sum_{p=u,c} V_{pb} V_{ps}^* \left\{ A_{K^{*-} \eta_q} \left[\delta_{pu} \alpha_2 + 2\alpha_3^p + \frac{1}{2} \alpha_{3,\text{EW}}^p \right] \right. \\ &\quad + \sqrt{2} A_{K^{*-} \eta_s} \left[\delta_{pu} \beta_2 + \alpha_3^p + \alpha_4^p - \frac{1}{2} \alpha_{3,\text{EW}}^p - \frac{1}{2} \alpha_{4,\text{EW}}^p + \beta_3^p + \beta_{3,\text{EW}}^p \right] \\ &\quad \left. + A_{\eta_q K^{*-}} \left[\delta_{pu} (\alpha_1 + \beta_2) + \alpha_4^p + \alpha_{4,\text{EW}}^p + \beta_3^p + \beta_{3,\text{EW}}^p \right] \right\}, \end{aligned} \quad (\text{A.3})$$

$$\begin{aligned} \sqrt{2} \mathcal{A}_{B^0 \rightarrow \phi \bar{K}^{*0}}^{\text{SM}} &= \sum_{p=u,c} V_{pb} V_{ps}^* \left\{ A_{\bar{K}^{*0} \eta_q} \left[\delta_{pu} \alpha_2 + 2\alpha_3^p + \frac{1}{2} \alpha_{3,\text{EW}}^p \right] \right. \\ &\quad + \sqrt{2} A_{\bar{K}^{*0} \eta_s} \left[\alpha_3^p + \alpha_4^p - \frac{1}{2} \alpha_{3,\text{EW}}^p - \frac{1}{2} \alpha_{4,\text{EW}}^p + \beta_3^p - \frac{1}{2} \beta_{3,\text{EW}}^p \right] \\ &\quad \left. + A_{\eta_q \bar{K}^{*0}} \left[\alpha_4^p - \frac{1}{2} \alpha_{4,\text{EW}}^p + \beta_3^p - \frac{1}{2} \beta_{3,\text{EW}}^p \right] \right\}, \end{aligned} \quad (\text{A.4})$$

where the explicit expressions for the coefficients $\alpha_i^p \equiv \alpha_i^p(M_1 M_2)$ and $\beta_i^p \equiv \beta_i^p(M_1 M_2)$ could also be found in ref. [23]. We recall that the α_i^p terms contain one-loop vertex, penguin and hard spectator contributions, whereas the β_i^p terms are due to the weak annihilation, and the transition form factors are encoded in the factors $A_{M_1 M_2}$.

The decay amplitude of $\bar{B}^0 \rightarrow \phi \bar{K}^{*0}$ mode can be read off from refs. [15, 16]

$$\mathcal{A}_{B^0 \rightarrow \phi \bar{K}^{*0}}^{\text{SM}} = A_{\bar{K}^{*0} \phi}^h \sum_{p=u,c} V_{pb} V_{ps}^* \left[\alpha_3^{p,h} + \alpha_4^{p,h} - \frac{1}{2} \alpha_{3,\text{EW}}^{p,h} - \frac{1}{2} \alpha_{4,\text{EW}}^{p,h} + \beta_3^{p,h} - \frac{1}{2} \beta_{3,\text{EW}}^{p,h} \right], \quad (\text{A.5})$$

where the superscript ‘ h ’ denotes the helicity of two final-state vector mesons, with $h = 0, +, -$ corresponding to two outgoing longitudinal, positive, and negative helicity vector mesons, respectively.

In the helicity basis, the decay amplitude eq. (A.5) can be further decomposed into the following three helicity amplitudes

$$H_{00}^{\text{SM}} = A_{\bar{K}^*0\phi}^0 \sum_{p=u,c} V_{pb}V_{ps}^* \left[\alpha_3^{p,0} + \alpha_4^{p,0} - \frac{1}{2}\alpha_{3,\text{EW}}^{p,0} - \frac{1}{2}\alpha_{4,\text{EW}}^{p,0} + \beta_3^{p,0} - \frac{1}{2}\beta_{3,\text{EW}}^{p,0} \right], \quad (\text{A.6})$$

$$H_{\pm\pm}^{\text{SM}} = A_{\bar{K}^*0\phi}^{\pm} \sum_{p=u,c} V_{pb}V_{ps}^* \left[\alpha_3^{p,\pm} + \alpha_4^{p,\pm} - \frac{1}{2}\alpha_{3,\text{EW}}^{p,\pm} - \frac{1}{2}\alpha_{4,\text{EW}}^{p,\pm} + \beta_3^{p,\pm} - \frac{1}{2}\beta_{3,\text{EW}}^{p,\pm} \right], \quad (\text{A.7})$$

with [15]

$$A_{\bar{K}^*0\phi}^h \equiv \frac{G_F}{\sqrt{2}} \langle \bar{K}^{*0} | (\bar{s}b)_{V-A} | \bar{B}^0 \rangle \langle \phi | (\bar{s}s)_{V-A} | 0 \rangle, \quad (\text{A.8})$$

$$A_{\bar{K}^*0\phi}^0 = \frac{iG_F}{\sqrt{2}} \frac{m_{B_d}^3 f_\phi}{2m_{K^*0}} \left[\left(1 + \frac{m_{K^*0}}{m_{B_d}}\right) A_1^{B \rightarrow K^*}(m_\phi^2) - \left(1 - \frac{m_{K^*0}}{m_{B_d}}\right) A_2^{B \rightarrow K^*}(m_\phi^2) \right], \quad (\text{A.9})$$

$$A_{\bar{K}^*0\phi}^{\pm} = \frac{iG_F}{\sqrt{2}} m_{B_d} m_\phi f_\phi \left[\left(1 + \frac{m_{K^*0}}{m_{B_d}}\right) A_1^{B \rightarrow K^*}(m_\phi^2) \mp \left(1 - \frac{m_{K^*0}}{m_{B_d}}\right) V^{B \rightarrow K^*}(m_\phi^2) \right]. \quad (\text{A.10})$$

B. Theoretical input parameters

B.1 Wilson coefficients and CKM matrix elements

The Wilson coefficients $C_i(\mu)$ have been evaluated reliably to next-to-leading logarithmic order [24, 44]. Their numerical results in the naive dimensional regularization scheme at the scale $\mu = m_b$ ($\mu_h = \sqrt{\Lambda_h m_b}$) are given by

$$\begin{aligned} C_1 &= 1.077 (1.178), & C_2 &= -0.174 (-0.355), & C_3 &= 0.013 (0.027), \\ C_4 &= -0.034 (-0.060), & C_5 &= 0.008 (0.011), & C_6 &= -0.039 (-0.081), \\ C_7/\alpha_{e.m.} &= -0.013 (-0.034), & C_8/\alpha_{e.m.} &= 0.047 (0.099), & C_9/\alpha_{e.m.} &= -1.208 (-1.338), \\ C_{10}/\alpha_{e.m.} &= 0.229 (0.426), & C_{7\gamma} &= -0.297 (-0.360), & C_{8g} &= -0.143 (-0.168). \end{aligned} \quad (\text{B.1})$$

The values at the scale μ_h , with $m_b = 4.79$ GeV and $\Lambda_h = 500$ MeV, should be used in the calculation of hard-spectator and weak annihilation contributions.

For the CKM matrix elements, we adopt the Wolfenstein parameterization [45] and choose the four parameters A , λ , ρ , and η as [46]

$$A = 0.809 \pm 0.014, \quad \lambda = 0.2272 \pm 0.0010, \quad \bar{\rho} = 0.197_{-0.030}^{+0.026}, \quad \bar{\eta} = 0.339_{-0.018}^{+0.019}, \quad (\text{B.2})$$

with $\bar{\rho} = \rho(1 - \frac{\lambda^2}{2})$ and $\bar{\eta} = \eta(1 - \frac{\lambda^2}{2})$.

B.2 Quark masses and lifetimes

As for the quark mass, there are two different classes appearing in our calculation. One type is the pole quark mass appearing in the evaluation of penguin loop corrections, and denoted by m_q . In this paper, we take

$$m_u = m_d = m_s = 0, \quad m_c = 1.64 \text{ GeV}, \quad m_b = 4.79 \text{ GeV}. \quad (\text{B.3})$$

The other one is the current quark mass which appears in the factor r_χ^M through the equation of motion for quarks. This type of quark mass is scale dependent and denoted by \overline{m}_q . Here we take [1]

$$\overline{m}_s(\mu)/\overline{m}_q(\mu) = 25 \sim 30, \quad \overline{m}_s(2 \text{ GeV}) = (95 \pm 25) \text{ MeV}, \quad \overline{m}_b(\overline{m}_b) = 4.20 \text{ GeV}, \quad (\text{B.4})$$

where $\overline{m}_q(\mu) = (\overline{m}_u + \overline{m}_d)(\mu)/2$, and the difference between u and d quark is not distinguished.

As for the lifetimes of B mesons, we take [1] $\tau_{B_u} = 1.638 \text{ ps}$, $\tau_{B_d} = 1.530 \text{ ps}$, and $\tau_{B_s} = 1.466 \text{ ps}$ as our default input values.

B.3 The decay constants and form factors

In this paper, we take the decay constants

$$\begin{aligned} f_B &= (216 \pm 22) \text{ MeV} [47], \quad f_{B_s} = (259 \pm 32) \text{ MeV} [47], \quad f_\pi = (130.7 \pm 0.4) \text{ MeV} [1], \\ f_K &= (159.8 \pm 1.5) \text{ MeV} [1] \quad f_{K^*} = (217 \pm 5) \text{ MeV} [48], \quad f_\phi = (231 \pm 4) \text{ MeV} [48], \\ f_{K^*}^\perp(1 \text{ GeV}) &= (185 \pm 10) \text{ MeV} [48], \quad f_\phi^\perp(1 \text{ GeV}) = (200 \pm 10) \text{ MeV} [48], \end{aligned} \quad (\text{B.5})$$

and the form factors [48]

$$\begin{aligned} F_0^{B \rightarrow \eta}(0) &= 0.275 \pm 0.036, & F_0^{B \rightarrow K}(0) &= 0.331 \pm 0.041, & A_0^{B \rightarrow K^*}(0) &= 0.374 \pm 0.033, \\ V^{B \rightarrow K^*}(0) &= 0.411 \pm 0.033, & A_1^{B \rightarrow K^*}(0) &= 0.292 \pm 0.028, & A_2^{B \rightarrow K^*}(0) &= 0.259 \pm 0.027, \\ V^{B_s \rightarrow \phi}(0) &= 0.434 \pm 0.035, & A_1^{B_s \rightarrow \phi}(0) &= 0.311 \pm 0.030, & A_2^{B_s \rightarrow \phi}(0) &= 0.234 \pm 0.028, \\ T_1^{B \rightarrow K^*}(0) &= 0.333 \pm 0.028, & T_2^{B \rightarrow K^*}(0) &= 0.333 \pm 0.028, & T_1^{B_s \rightarrow \phi}(0) &= 0.349 \pm 0.033, \\ T_2^{B_s \rightarrow \phi}(0) &= 0.349 \pm 0.033. \end{aligned}$$

For the parameters related to the η - η' mixing, we choose [28]

$$f_q = (1.07 \pm 0.02) f_\pi, \quad f_s = (1.34 \pm 0.06) f_\pi, \quad \phi = 39.3^\circ \pm 1.0^\circ. \quad (\text{B.6})$$

The other parameters relevant to the meson η can be obtained from the above three ones [9].

B.4 The LCDAs of mesons

For the LCDAs of mesons, we use their asymptotic forms [36, 38]

$$\begin{aligned} \Phi_P(x) &= \Phi_{\parallel, \perp}^V(x) = g_\perp^{(a)V}(x) = 6x(1-x), \quad \Phi_P(x) = 1, \\ \Phi_v(x) &= 3(2x-1), \quad g_\perp^{(v)V}(x) = \frac{3}{4} [1 + (2x-1)^2]. \end{aligned} \quad (\text{B.7})$$

As for the B meson wave functions, we need only consider the first inverse moment of the leading LCDA $\Phi_1^B(\xi)$ defined by [22]

$$\int_0^1 \frac{d\xi}{\xi} \Phi_1^B(\xi) \equiv \frac{m_B}{\lambda_B}, \quad (\text{B.8})$$

where $\lambda_B = (460 \pm 110) \text{ MeV}$ [49] is the hadronic parameter introduced to parameterize this integral.

References

- [1] PARTICLE DATA GROUP collaboration, W.M. Yao et al., *Review of particle physics*, *J. Phys.* **G 33** (2006) 1.
- [2] HEAVY FLAVOR AVERAGING GROUP (HFAG) collaboration, E. Barberio et al., *Averages of B-hadron properties at the end of 2005*, hep-ex/0603003, and online update at: <http://www.slac.stanford.edu/xorg/hfag>.
- [3] H.J. Lipkin, *CP-violation difference in B^0 and B^\pm decays explained: no tree-penguin interference in $B^+ \rightarrow K^+ \pi_0$* , hep-ph/0608284;
S. Khalil, *Supersymmetric contributions to $B \rightarrow K\pi$ in the view of recent experimental result*, hep-ph/0608157;
M. Gronau and J.L. Rosner, *Rate and CP-asymmetry sum rules in $B \rightarrow K\pi$* , *Phys. Rev.* **D 74** (2006) 057503 [hep-ph/0608040];
S. Baek, *New physics in $B \rightarrow \pi\pi$ and $B \rightarrow \pi K$ decays*, *JHEP* **07** (2006) 025 [hep-ph/0605094];
R. Arnowitt, B. Dutta, B. Hu and S. Oh, *The $B \rightarrow K\pi$ puzzle and supersymmetric models*, *Phys. Lett.* **B 633** (2006) 748 [hep-ph/0509233];
H.-n. Li, S. Mishima and A.I. Sanda, *Resolution to the $b \rightarrow pi k$ puzzle*, *Phys. Rev.* **D 72** (2005) 114005 [hep-ph/0508041];
X.-q. Li and Y.-d. Yang, *Revisiting $B \rightarrow \pi\pi$, πK decays in QCD factorization approach*, *Phys. Rev.* **D 72** (2005) 074007 [hep-ph/0508079];
C.S. Kim, S. Oh and C. Yu, *A critical study of the $B \rightarrow K\pi$ puzzle*, *Phys. Rev.* **D 72** (2005) 074005 [hep-ph/0505060];
S. Khalil, *CP asymmetries and branching ratios of $B \rightarrow K\pi$ in supersymmetric models*, *Phys. Rev.* **D 72** (2005) 035007 [hep-ph/0505151].
- [4] CLEO collaboration, S.J. Richichi et al., *Two-body B meson decays to η and η' : observation of $B \rightarrow \eta K^*$* , *Phys. Rev. Lett.* **85** (2000) 520 [hep-ex/9912059].
- [5] BABAR collaboration, B. Aubert et al., *Measurement of branching fractions and charge asymmetries in b^+ decays to $\eta\pi^+$, ηk^+ , $\eta\rho^+$ and $\eta'\pi^+$ and search for B^0 decays to ηk^0 and $\eta\omega$* , *Phys. Rev. Lett.* **95** (2005) 131803 [hep-ex/0503035];
BABAR collaboration, B. Aubert et al., *Searches for B^0 decays to ηK^0 , $\eta\eta$, $\eta'\eta'$, $\eta\phi$ and $\eta'\phi$* , *Phys. Rev.* **D 74** (2006) 051106 [hep-ex/0607063].
- [6] BELLE collaboration, K. Abe et al., *Improved measurements of branching fractions and CP asymmetries in $B \rightarrow \eta H$ decays*, *Phys. Rev.* **D 75** (2007) 071104 [hep-ex/0608033];
K. Abe et al., *Measurement of charmless B decays to ηK^* and $\eta\rho$* , hep-ex/0608034.
- [7] H.J. Lipkin, *Analysis of new charmless strange B decay data leaves high $B \rightarrow K\eta'$ and $B \rightarrow K\eta'x$ still unexplained*, *Phys. Lett.* **B 633** (2006) 540 [hep-ph/0507225];
A.R. Williamson and J. Zupan, *Two body B decays with isosinglet final states in SCET*, *Phys. Rev.* **D 74** (2006) 014003 [hep-ph/0601214];
J.-F. Cheng, C.-S. Huang and X.-H. Wu, *CP asymmetries in $B \rightarrow \phi K_s$ and $B \rightarrow \eta' k_s$ in MSSM*, *Nucl. Phys.* **B 701** (2004) 54 [hep-ph/0404055];
B. Dutta, C.S. Kim, S. Oh and G.-h. Zhu, *An analysis of $B \rightarrow \eta' K$ decays using a global fit in QCD factorization*, *Eur. Phys. J.* **C 37** (2004) 273 [hep-ph/0312388];
B. Dutta, C.S. Kim and S. Oh, *A consistent resolution of possible anomalies in $B^0 \rightarrow \phi K_s$ and $B^+ \rightarrow \eta' k^+$ decays*, *Phys. Rev. Lett.* **90** (2003) 011801 [hep-ph/0208226];

- C.-W. Chiang, M. Gronau and J.L. Rosner, *Two-body charmless B decays involving η and η'* , *Phys. Rev. D* **68** (2003) 074012 [[hep-ph/0306021](#)];
- A. Kundu and T. Mitra, *Simultaneous solution to $B \rightarrow \phi K$ CP asymmetry and $B \rightarrow \eta' K$, $B \rightarrow \eta K^*$ branching ratio anomalies from R-parity violation*, *Phys. Rev. D* **67** (2003) 116005 [[hep-ph/0302123](#)];
- E. Kou and A.I. Sanda, *$B \rightarrow K\eta'$ decay in perturbative QCD*, *Phys. Lett. B* **525** (2002) 240 [[hep-ph/0106159](#)];
- D.-s. Du, D.-s. Yang and G.-h. Zhu, *Further analysis of di-gluon fusion mechanism for the decays of $B \rightarrow K\eta'$* , [hep-ph/9912201](#);
- D.-s. Du, C.S. Kim and Y.-d. Yang, *A new mechanism for $B^\pm \rightarrow \eta' K^\pm$ in perturbative QCD*, *Phys. Lett. B* **426** (1998) 133 [[hep-ph/9711428](#)].
- [8] M.-Z. Yang and Y.-D. Yang, *Crucial study of charmless two-body B decays involving η' and η* , *Nucl. Phys. B* **609** (2001) 469 [[hep-ph/0012208](#)].
- [9] M. Beneke and M. Neubert, *Flavor-singlet B decay amplitudes in QCD factorization*, *Nucl. Phys. B* **651** (2003) 225 [[hep-ph/0210085](#)].
- [10] A. Kundu, S. Nandi and J.P. Saha, *New physics in $B \rightarrow S\bar{S}S$ decay*, *Phys. Lett. B* **622** (2005) 102 [[hep-ph/0504173](#)].
- [11] BABAR collaboration, B. Aubert et al., *Rates, polarizations and asymmetries in charmless vector-vector B meson decays*, *Phys. Rev. Lett.* **91** (2003) 171802 [[hep-ex/0307026](#)]; *Measurement of the $B^0 \rightarrow \phi K^0$ decay amplitudes*, *Phys. Rev. Lett.* **93** (2004) 231804 [[hep-ex/0408017](#)].
- [12] BELLE collaboration, K.F. Chen et al., *Measurement of polarization and triple-product correlations in $B \rightarrow \phi K^*$ decays*, *Phys. Rev. Lett.* **94** (2005) 221804 [[hep-ex/0503013](#)].
- [13] P. Bussey (CDF Collaboration), talk given at the ICHEP (2006).
- [14] C.-H. Chen and H. Hatanaka, *Nonuniversal Z' couplings in B decays*, *Phys. Rev. D* **73** (2006) 075003 [[hep-ph/0602140](#)];
- C.-S. Huang, P. Ko, X.-H. Wu and Y.-D. Yang, *MSSM anatomy of the polarization puzzle in $B \rightarrow \phi K^*$ decays*, *Phys. Rev. D* **73** (2006) 034026 [[hep-ph/0511129](#)];
- S. Baek, A. Datta, P. Hamel, O.F. Hernandez and D. London, *Polarization states in $B \rightarrow \rho K^*$ and new physics*, *Phys. Rev. D* **72** (2005) 094008 [[hep-ph/0508149](#)];
- Y.-D. Yang, R.-M. Wang and G.-R. Lu, *Polarizations in decays $B_{u,d} \rightarrow vv$ and possible implications for R-parity violating SUSY*, *Phys. Rev. D* **72** (2005) 015009 [[hep-ph/0411211](#)];
- H.-n. Li and S. Mishima, *Polarizations in $B \rightarrow vv$ decays*, *Phys. Rev. D* **71** (2005) 054025 [[hep-ph/0411146](#)];
- C.-H. Chen and C.-Q. Geng, *Scalar interactions to the polarizations of $B \rightarrow \phi K^*$* , *Phys. Rev. D* **71** (2005) 115004 [[hep-ph/0504145](#)];
- H.-Y. Cheng, C.-K. Chua and A. Soni, *Final state interactions in hadronic B decays*, *Phys. Rev. D* **71** (2005) 014030 [[hep-ph/0409317](#)];
- H.-n. Li, *Resolution to the $B \rightarrow \phi K^*$ polarization puzzle*, *Phys. Lett. B* **622** (2005) 63 [[hep-ph/0411305](#)];
- P. Colangelo, F. De Fazio and T.N. Pham, *The riddle of polarization in $B \rightarrow vv$ transitions*, *Phys. Lett. B* **597** (2004) 291 [[hep-ph/0406162](#)];
- M. Ladisa, V. Laporta, G. Nardulli and P. Santorelli, *Final state interactions for $B \rightarrow vv$ charmless decays*, *Phys. Rev. D* **70** (2004) 114025 [[hep-ph/0409286](#)];
- E. Alvarez, L.N. Epele, D.G. Dumm and A. Szyrkman, *Right handed currents and FSI phases in $B^0 \rightarrow \phi K_0^*$* , *Phys. Rev. D* **70** (2004) 115014 [[hep-ph/0410096](#)];

- C. Dariescu, M.A. Dariescu, N.G. Deshpande and D.K. Ghosh, *CP-violating SUSY effects in penguin dominated modes $B \rightarrow \phi K$ and $B \rightarrow \phi K^*$* , *Phys. Rev.* **D 69** (2004) 112003 [[hep-ph/0308305](#)].
- [15] M. Beneke, J. Rohrer and D. Yang, *Enhanced electroweak penguin amplitude in $B \rightarrow vv$ decays*, *Phys. Rev. Lett.* **96** (2006) 141801 [[hep-ph/0512258](#)].
- [16] M. Beneke, J. Rohrer and D. Yang, *Branching fractions, polarisation and asymmetries of $B \rightarrow vv$ decays*, [hep-ph/0612290](#).
- [17] A.L. Kagan, *Polarization in $B \rightarrow vv$ decays*, *Phys. Lett.* **B 601** (2004) 151 [[hep-ph/0405134](#)].
- [18] P.K. Das and K.-C. Yang, *Data for polarization in charmless $B \rightarrow \phi K^*$: a signal for new physics?*, *Phys. Rev.* **D 71** (2005) 094002 [[hep-ph/0412313](#)].
- [19] C.S. Kim and Y.-D. Yang, *Polarization anomaly in $B \rightarrow \phi K^*$ and probe of tensor interactions*, [hep-ph/0412364](#).
- [20] S. Nandi and A. Kundu, *New physics in $b \rightarrow s\bar{s}s$ decay. II: Study of $B \rightarrow V(1)V(2)$ modes*, *J. Phys.* **G 32** (2006) 835.
- [21] Y.-Y. Charng, T. Kurimoto and H.-N. Li, *Gluonic contribution to $B \rightarrow \eta'$ form factors*, *Phys. Rev.* **D 74** (2006) 074024 [[hep-ph/0609165](#)];
C.-H. Chen and C.-Q. Geng, *η' productions in semileptonic B decays*, *Phys. Lett.* **B 645** (2007) 197 [[hep-ph/0608246](#)].
- [22] M. Beneke, G. Buchalla, M. Neubert and C.T. Sachrajda, *QCD factorization for $B \rightarrow \pi\pi$ decays: strong phases and CP-violation in the heavy quark limit*, *Phys. Rev. Lett.* **83** (1999) 1914 [[hep-ph/9905312](#)]; *QCD factorization for exclusive, non-leptonic b meson decays: general arguments and the case of heavy-light final states*, *Nucl. Phys.* **B 591** (2000) 313 [[hep-ph/0006124](#)]; *QCD factorization in $B \rightarrow \pi K, \pi\pi$ decays and extraction of Wolfenstein parameters*, *Nucl. Phys.* **B 606** (2001) 245 [[hep-ph/0104110](#)].
- [23] M. Beneke and M. Neubert, *QCD factorization for $b \rightarrow pp$ and $B \rightarrow pv$ decays*, *Nucl. Phys.* **B 675** (2003) 333 [[hep-ph/0308039](#)].
- [24] G. Buchalla, A.J. Buras and M.E. Lautenbacher, *Weak decays beyond leading logarithms*, *Rev. Mod. Phys.* **68** (1996) 1125 [[hep-ph/9512380](#)].
- [25] N. Cabibbo, *Unitary symmetry and leptonic decays*, *Phys. Rev. Lett.* **10** (1963) 531;
M. Kobayashi and T. Maskawa, *CP-violation in the renormalizable theory of weak interaction*, *Prog. Theor. Phys.* **49** (1973) 652.
- [26] X.-Q. Li and Y.-D. Yang, *Reexamining charmless $B \rightarrow pv$ decays in QCD factorization approach*, *Phys. Rev.* **D 73** (2006) 114027 [[hep-ph/0602224](#)].
- [27] T. Feldmann and T. Hurth, *Non-factorizable contributions to $B \rightarrow \pi\pi$ decays*, *JHEP* **11** (2004) 037 [[hep-ph/0408188](#)].
- [28] T. Feldmann, P. Kroll and B. Stech, *Mixing and decay constants of pseudoscalar mesons*, *Phys. Rev.* **D 58** (1998) 114006 [[hep-ph/9802409](#)]; *Mixing and decay constants of pseudoscalar mesons: the sequel*, *Phys. Lett.* **B 449** (1999) 339 [[hep-ph/9812269](#)];
T. Feldmann, *Quark structure of pseudoscalar mesons*, *Int. J. Mod. Phys.* **A 15** (2000) 159 [[hep-ph/9907491](#)].
- [29] R. Escribano and J.-M. Frere, *Study of the $\eta\eta'$ system in the two mixing angle scheme*, *JHEP* **06** (2005) 029 [[hep-ph/0501072](#)].

- [30] J.-F. Cheng, C.-S. Huang and X.-H. Wu, *Neutral Higgs boson contributions to CP asymmetry of $B \rightarrow \phi K_s$ in MSSM*, *Phys. Lett. B* **585** (2004) 287 [[hep-ph/0306086](#)]; C.S. Huang et al., in ref. [14].
- [31] G. Hiller and F. Kruger, *More model-independent analysis of $B \rightarrow S$ processes*, *Phys. Rev. D* **69** (2004) 074020 [[hep-ph/0310219](#)].
- [32] E. Frlez et al., *Precise measurement of the pion axial form factor in the $\pi^+ \rightarrow e^+ \nu \gamma$ decay*, *Phys. Rev. Lett.* **93** (2004) 181804 [[hep-ex/0312029](#)].
- [33] A.A. Poblaguev, *On the analysis of the $\pi \rightarrow e \nu \gamma$ experimental data*, *Phys. Rev. D* **68** (2003) 054020 [[hep-ph/0307166](#)]; *On the $\pi \rightarrow e$ neutrino gamma decay sensitivity to a tensor coupling in the effective quark lepton interaction*, *Phys. Lett. B* **238** (1990) 108.
- [34] M.V. Chizhov, *New tensor particles from $\pi \rightarrow e \nu \gamma$ and $K \rightarrow \pi e \nu$ decays*, *Mod. Phys. Lett. A* **8** (1993) 2753 [[hep-ph/0401217](#)]; *Search for tensor interactions in kaon decays at $d\Phi ne$* , *Phys. Lett. B* **381** (1996) 359 [[hep-ph/9511287](#)].
- [35] P. Herczeg, *On the question of a tensor interaction in $\pi \rightarrow e$ electron-neutrino gamma decay*, *Phys. Rev. D* **49** (1994) 247; M.B. Voloshin, *Upper bound on tensor interaction in the decay $\pi^- \rightarrow e^-$ anti-neutrino gamma*, *Phys. Lett. B* **283** (1992) 120.
- [36] M. Beneke and T. Feldmann, *Symmetry-breaking corrections to heavy-to-light B meson form factors at large recoil*, *Nucl. Phys. B* **592** (2001) 3 [[hep-ph/0008255](#)].
- [37] M. Wirbel, B. Stech and M. Bauer, *Exclusive semileptonic decays of heavy mesons*, *Z. Physik C* **29** (1985) 637; *Exclusive nonleptonic decays of D , D_s and B mesons*, *Z. Physik C* **34** (1987) 103.
- [38] A. Ali, P. Ball, L.T. Handoko and G. Hiller, *A comparative study of the decays $B \rightarrow (K, K^*) \ell^+ \ell^-$ in standard model and supersymmetric theories*, *Phys. Rev. D* **61** (2000) 074024 [[hep-ph/9910221](#)]; P. Ball and V.M. Braun, *Exclusive semileptonic and rare B meson decays in QCD*, *Phys. Rev. D* **58** (1998) 094016 [[hep-ph/9805422](#)]; P. Ball, V.M. Braun, Y. Koike and K. Tanaka, *Higher twist distribution amplitudes of vector mesons in QCD: formalism and twist three distributions*, *Nucl. Phys. B* **529** (1998) 323 [[hep-ph/9802299](#)].
- [39] A. Datta and D. London, *Triple-product correlations in $B \rightarrow v_1 v_2$ decays and new physics*, *Int. J. Mod. Phys. A* **19** (2004) 2505 [[hep-ph/0303159](#)]; D. London, N. Sinha and R. Sinha, *Bounds on new physics from $B \rightarrow v_1 v_2$ decays*, *Phys. Rev. D* **69** (2004) 114013 [[hep-ph/0402214](#)]; K. Abe, M. Satpathy and H. Yamamoto, *Time-dependent angular analyses of B decays*, [hep-ex/0103002](#); I. Dunietz, H.R. Quinn, A. Snyder, W. Toki and H.J. Lipkin, *How to extract CP-violating asymmetries from angular correlations*, *Phys. Rev. D* **43** (1991) 2193.
- [40] C.M. Arnesen, Z. Ligeti, I.Z. Rothstein and I.W. Stewart, *Power corrections in charmless nonleptonic B decays: annihilation is factorizable and real*, [hep-ph/0607001](#) and references therein; C.M. Arnesen, I.Z. Rothstein and I.W. Stewart, *Three-parton contributions to $B \rightarrow M_1 M_2$ annihilation at leading order*, *Phys. Lett. B* **647** (2007) 405 [[hep-ph/0611356](#)].

- [41] A. Datta et al., *Methods for measuring new-physics parameters in B decays*, *Phys. Rev. D* **71** (2005) 096002 [[hep-ph/0406192](#)];
A. Datta and D. London, *Measuring new-physics parameters in B penguin decays*, *Phys. Lett. B* **595** (2004) 453 [[hep-ph/0404130](#)].
- [42] X.Q. Li, G.-R. Lu and Y.D. Yang, *Charmless $\bar{B}_s \rightarrow vv$ decays in QCD factorization*, *Phys. Rev. D* **68** (2003) 114015 [[hep-ph/0309136](#)];
Y.-H. Chen, H.-Y. Cheng and B. Tseng, *Charmless hadronic two-body decays of the B_s mesons*, *Phys. Rev. D* **59** (1999) 074003 [[hep-ph/9809364](#)].
- [43] A. Ali et al., *Charmless non-leptonic B_s decays to pp , pv and vv final states in the PQCD approach*, [hep-ph/0703162](#).
- [44] A.J. Buras, P. Gambino and U.A. Haisch, *Electroweak penguin contributions to non-leptonic $\Delta F = 1$ decays at NNLO*, *Nucl. Phys. B* **570** (2000) 117 [[hep-ph/9911250](#)].
- [45] L. Wolfenstein, *Parametrization of the Kobayashi-Maskawa matrix*, *Phys. Rev. Lett.* **51** (1983) 1945.
- [46] CKMFITTER GROUP collaboration, J. Charles et al., *CP-violation and the ckm matrix: assessing the impact of the asymmetric B factories*, *Eur. Phys. J. C* **41** (2005) 1 [[hep-ph/0406184](#)]; updated results and plots available at: <http://ckmfitter.in2p3.fr>.
- [47] HPQCD collaboration, A. Gray et al., *The B meson decay constant from unquenched lattice QCD*, *Phys. Rev. Lett.* **95** (2005) 212001 [[hep-lat/0507015](#)].
- [48] P. Ball and R. Zwicky, *New results on $B \rightarrow \pi, K, \eta$ decay formfactors from light-cone sum rules*, *Phys. Rev. D* **71** (2005) 014015 [[hep-ph/0406232](#)]; *SU(3) breaking of leading-twist K and K^* distribution amplitudes: a reprise*, *Phys. Lett. B* **633** (2006) 289 [[hep-ph/0510338](#)].
- [49] V.M. Braun, D.Y. Ivanov and G.P. Korchemsky, *The B-meson distribution amplitude in QCD*, *Phys. Rev. D* **69** (2004) 034014 [[hep-ph/0309330](#)];
A. Khodjamirian, T. Mannel and N. Offen, *B-meson distribution amplitude from the $B \rightarrow \pi$ form factor*, *Phys. Lett. B* **620** (2005) 52 [[hep-ph/0504091](#)].